

# Angular dependence of mammographic dosimeters in digital breast tomosynthesis

Lena R. Bradley, Ann-Katherine Carton, Andrew D.A. Maidment

Department of Radiology, University of Pennsylvania, 3400 Spruce Street, Philadelphia, PA 19104

Lena.Bradley@psu.edu, {Ann-Katherine.Carton | Andrew.Maidment}@uphs.upenn.edu

## ABSTRACT

Digital Breast Tomosynthesis (DBT) is an emerging imaging modality that combines tomography with conventional digital mammography. In developing DBT dosimetry, a direct application of mammographic dosimetry has appeal. However, DBT introduces rotation of the x-ray tube relative to the dosimeter, thus raising questions about the angular dependence of mammographic dosimeters. To measure this dependence, two ionization chambers, two solid-state detectors, and one photodiode were rotated relative to an incident Mo/Mo x-ray beam. In this isocentric DBT simulation, the signal of each dosimeter was studied over an angular range of  $180^\circ$  for tube voltages of 26 to 34 kV. One ionization chamber was then modeled numerically to study the response to various monoenergetic beams. The results show that all dosimeters underestimate dose to varying degrees; solid-state detectors show the greatest angular dependence while ionization chambers show the least. Correction factors were computed from the data for isocentric DBT images using projection angles up to  $\pm 25^\circ$ ; these factors ranged from 1.0014 to 1.1380. The magnitude of the angular dependence generally decreased with increasing energy, as shown with both the measured and modeled data. As a result, the error arising in measuring DBT dose with a mammographic dosimeter varies significantly; it cannot always be disregarded. The use of correction factors may be possible but is largely impractical, as they are specific to the dosimeter, x-ray beam, and DBT geometry. Instead, an angle-independent dosimeter may be more suitable for DBT.

**Keywords:** digital breast tomosynthesis, dosimetry, radiation dose, ionization chamber, solid-state detector, photodiode

## 1. INTRODUCTION

Digital breast tomosynthesis (DBT) is an imaging modality in which the x-ray tube rotates around a stationary breast support and compression device, producing low dose projection images. These projections, collected at multiple angles, are reconstructed into three-dimensional slices<sup>1</sup>. Preliminary studies show that DBT has improved sensitivity and specificity over two-dimensional digital mammography<sup>2</sup>. DBT thus lowers the likelihood for superposition of dense fibroglandular tissue over a tumor, allowing for improved cancer detection. When DBT becomes clinically available, accurate dosimetry and quality assurance will be required. Presently, however, there are no standard procedures or dosimeters specific to the modality; instead, it is common to use mammographic dosimeters and dosimetry techniques.

Mammographic dosimetry is generally performed using either solid-state detectors or parallel-plate ionization chambers. These dosimeters are specifically designed to collect radiation which is incident normal to the face of the device. In mammography, they are normally held parallel to and slightly above the breast support. The IAEA *Dosimetry in Diagnostic Radiology: An International Code of Practice*<sup>3</sup> specifies that ionization chambers should be oriented with the plates perpendicular to the beam axis, and that the signal generated in semiconductor dosimeters may also depend on their orientation relative to the incident beam. In mammography, the dosimeter and x-ray tube are held fixed relative to the breast support, thus avoiding most angular concerns beyond small set-up errors. However, as the x-ray tube rotates around the breast support in DBT, large angular variation is introduced between the tube and dosimeter, thus violating the Code of Practice. If mammographic dosimeters are to be transitioned to DBT appropriately, then the effects of the changing angle of incident radiation must be well understood.

In this work, an investigation was performed to study the angular dependence of common mammography dosimeters in DBT geometries. Various ionization chambers and solid-state dosimeters were tested for signal dependence when rotated in a mammographic x-ray beam. These trends were observed over a range of tube voltages. One ionization chamber was modeled numerically to study the effects of tube target and filtration. Using these results, DBT exams were simulated, producing correction factors that could possibly allow the dosimeters to be used in such geometries.

## 2. MATERIALS AND METHODS

### 2.1 Dosimeters

Five mammographic dosimeters, including two ionization chambers, two solid-state detectors and one photodiode, were studied to measure the dependence of the signal on the angle of the incident radiation. The ionization chambers used (Model 96035B, Fluke Biomedical, Cleveland, OH and Model 1515-6M, Radcal Corporation, Monrovia, California) are both vented volume, parallel plate air chambers. They collect x-rays from cylindrical active-air volumes of 15 cc and 6 cc, respectively. The 96035B ionization chamber has two different entrance windows; only the window intended for mammography was used.

Two solid-state detectors (Barracuda MPD and R100B, RTI Electronics, Mölndal, Sweden) were tested. The Barracuda MPD collects x-rays using an array of five small solid-state detectors, depicted in Figure 1. The device incorporates mechanical filters to analyze beam energy and half value layer. Due to the linear construction of the individual detectors inside, the Barracuda MPD was rotated in two perpendicular geometries: vertical and horizontal. In the vertical alignment, the Barracuda MPD axis of rotation corresponded with the axis along which the five chips are aligned, while for the horizontal alignment, these two axes were perpendicular. The Barracuda R100B, has just one sensor and thus requires only one rotational geometry. Both Barracuda dosimeters have lead shields on the back and sides to control backscatter.

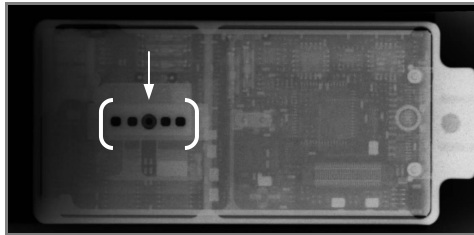


**Figure 1.** High energy x-ray image showing internal structure of Barracuda MPD. The linear array of five solid-state detectors is seen in the center-left.

A photodiode (Model RZ 1002/21, Ziehm Imaging, Nürnberg, Germany), extracted from an early mammographic automatic exposure control, was also tested. The photodiode is approximately semicircular, with a diameter of 7.54 cm, and a depth of 0.88 cm. Due to the photodiode's high sensitivity, 2 mm of Al filtration was added to the beam before collimation in order to reduce the signal.

### 2.2 Experimental geometry

An isocentric DBT system was simulated to test the angular dependence of the mammographic dosimeters. As in Figure 2, each dosimeter was aligned with its active front face centered in the beam; the dosimeter was rotated relative to this beam. The geometry was defined such that, at  $0^\circ$ , the radiation was perpendicularly incident on the front face, while at  $\pm 90^\circ$  the radiation was incident on the edge of the dosimeter. The reference to positive and negative angles is arbitrary due to the symmetric geometry, but nonetheless remained consistent throughout.

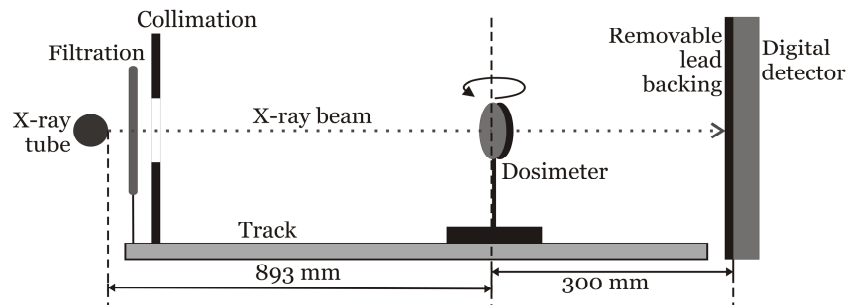


**Figure 2.** Experimental geometry used to simulate an isocentric DBT system. The dosimeter is rotated relative to the central ray of the beam, leaving the x-ray tube, filters and collimator stationary.

A mammographic x-ray tube (M51, General Electric Health Care, Chalfont St. Giles, UK) with a Mo target and  $30\ \mu\text{m}$  of added Mo filtration was operated at 50 mAs. The tube was positioned on an optical bench aligned with an optical rail.

A laser, aligned with the central x-ray beam, was used to position each dosimeter before testing. The dosimeter itself was mounted on a rotation stage so that the angle of rotation could be accurately controlled. The dosimeters' axis of rotation was located 893 mm from the tube focus, a value that was confirmed using a least-squares inverse-square fit of the readings at varying tube-dosimeter distances.

In order to minimize backscatter, a rectangular lead aperture of adjustable dimensions was used to collimate the beam tightly around each dosimeter while still irradiating the entire device. A digital detector placed behind the dosimeter was used to record and adjust the collimation, as shown in Figure 3. After collimation had been set, a lead backing was inserted just in front of the detector.

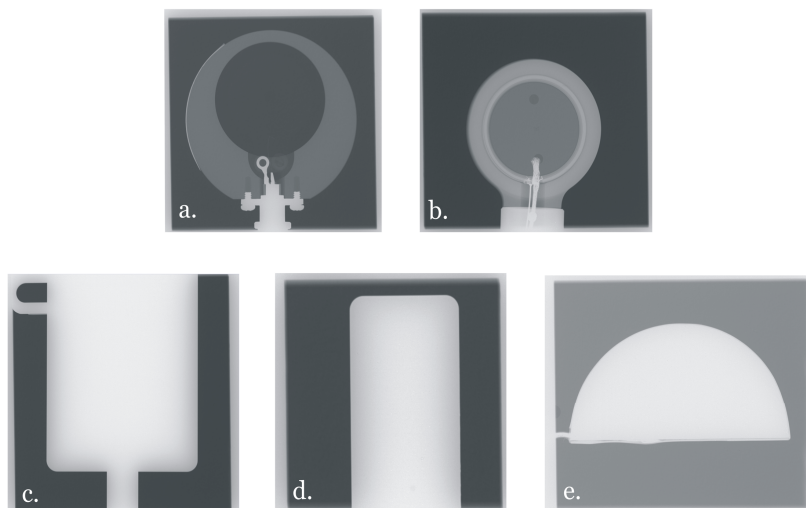


**Figure 3.** Images from the digital detector showing collimation for dosimeter a) 96035B, b) 1515-6M, c) Barracuda MPD in vertical orientation, d) Barracuda R100B, and e) RZ 1002/21. Note that RZ 1002/21 was exposed with 2mm of Al added to the beam.

The angular dependence of each dosimeter was first tested in  $5^\circ$  increments over  $\pm 90^\circ$  from normal incidence, in response to a 28 kV x-ray beam. The dosimeter was stopped at each angular position and three readings, taken in 30-second intervals, were averaged before moving to the next position.

The angular dependence was also measured for various beam energies in a similar fashion. Because DBT generally uses a limited range of angles, a smaller angular range was chosen for measuring the kV dependence. Only five positions, spaced equally within this smaller range, were used to analyze the trends. For each dosimeter, three measurements from each angular position were averaged and measurements were repeated over the new angular range for tube voltages of 26 to 34 kV. For each beam energy, the measurement at each angle was normalized to the appropriate measurement at perpendicular incidence.

### 2.3 Ion Chamber Model

Rotation of the x-ray tube relative to the dosimeter in DBT has the effect of altering the material found in the path between the x-ray source and a given point in the dosimeter, thus changing the attenuation of the x-ray beam between these two points. The angular dependence of the dosimeter is therefore expected to result largely from this varying attenuation.

A numerical model of the 96035B ionization chamber was developed in order to simulate changes in attenuation as a function of the incidence angle. The cylindrical active air volume of the ion chamber is surrounded by a non-concentric cylindrical wall and covered with a thin window. Based on the specifications provided,<sup>4</sup> the 15 cc active air volume was segmented into seven radial divisions, forty angular divisions, and five depth divisions, yielding a total of 1400 voxels. The voxels ranged in size from 1.53 to 19.93 mm<sup>3</sup> for a total modeled volume of 15026 mm<sup>3</sup>. The x-ray beam was assumed to originate from a monoenergetic point source that rotated around the center point of the active volume's top face. This geometry is depicted in Figure 4.

To model the experimental results at 28 kV, the relative air kerma was calculated at the center point of each voxel based on the inverse square law and the energy-dependent attenuation from material in the beam. The kerma for all points was

weighted by voxel volume and then summed for each angle of rotation. The model was used to simulate monoenergetic beams of varying energy to study the angular dependence as a function of energy.

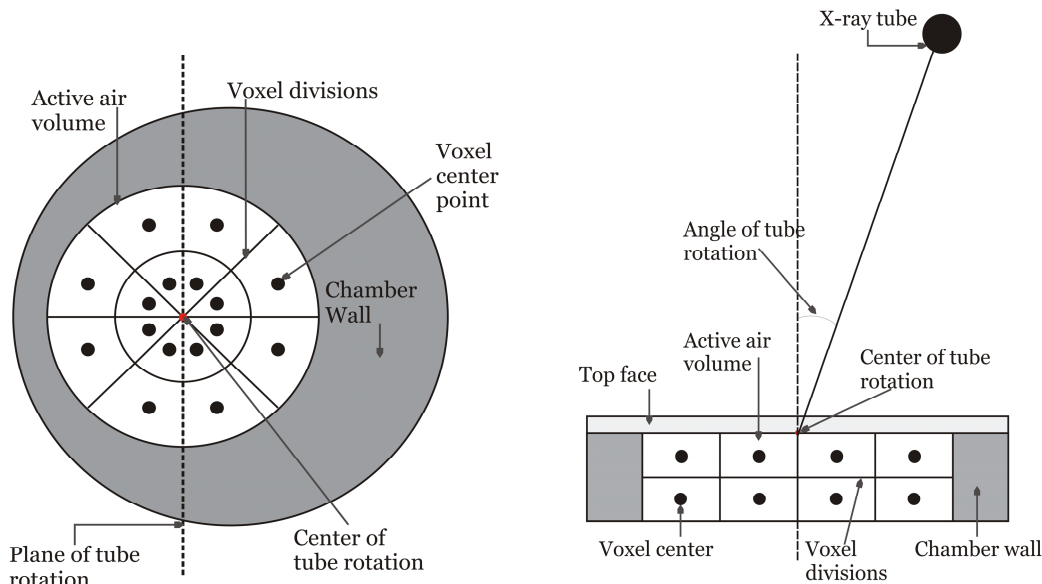


**Figure 4.** Geometry of Fluke 96035B model and voxelization as viewed from the top and side. For illustration purposes, the active volume is shown with two radial divisions, eight angular divisions, and two depth divisions for a total of 32 voxels.

## 2.4 Analysis of angular dependence

Using the experimental results from measurements taken at 28 kV, polynomial least-squares fits of order 2 through 8 were applied to the data from each dosimeter. Equation 1 was used to compute an  $n^{\text{th}}$ -order polynomial.

$$y = \sum_{j=1}^n C_j x^j \quad (1)$$

Here,  $x$  is the angle of incidence,  $y$  is the dosimeter response, and values of  $C_j$  were varied to achieve the best fit.

The most appropriate fit was chosen based on the coefficients of determination. This was then used to compute correction factors necessary for accurate dosimetry in an isocentric DBT exam of varying number and angular range of views. The calculations assume that, in a 28 kV Mo/Mo beam, each tomosynthesis view was obtained with the same mAs as the view taken at normal incidence. Further, the views were assumed to be taken in a “stop-and-go” manner at fixed angles, distributed evenly over the angular range used.

Based on the polynomial fit, isocentric correction factors,  $f_{iso}$ , were computed as the ratio of total dose received at the center of the dosimeter face to the total dose measured by the dosimeter at the various angles. Equation 2 was used to produce these factors.

$$f_{iso} = \frac{S_{\perp} N}{S_{\perp} + 2 \sum_{k=1}^{\frac{1}{2}(N-1)} S(\alpha)} \quad (2)$$

$$\alpha = \left( \frac{2kR}{N-1} \right) \quad (3)$$

Here,  $N$  is the number of individual tomosynthesis views and  $R$  is the angular range of views, as in  $\pm R^{\circ}$  from normal incidence.  $S_{\perp}$  is the fitted value at normal incidence, and  $S(\alpha)$  is the fitted value at angle  $\alpha$ . The tomosynthesis angle,  $\alpha$ , is a function of  $R$  and  $N$  and indicates the angle of rotation relative to the x-ray tube.

## 2.5 Analysis of energy dependence

Because the angular dependence of the dosimeter signal is largely due to the variation in the attenuating materials in the x-ray beam as a function of angle, and because x-rays are generally more penetrating at higher energies, the energy dependence of the experimental data was tested. At a higher kV, the signal from the dosimeters should show less angular dependence because high energy x-rays are less attenuated by the chamber wall and top materials. Therefore, at given angle, pairs of normalized mean readings at different kV were compared, assuming normal distributions with similar standard deviations. Significant differences were analyzed at the 0.05 level using a paired, two-sided Student's *t*-test under the null hypothesis that the distribution of differences in the normalized means is symmetric about zero. Additionally, a binomial counting test was performed to analyze how often, at a given extreme angle, the lower normalized value would correspond to the lower beam quality.

## 3. RESULTS

### 3.1 Angular dependence

The signal from each of the five dosimeters was measured at finely spaced angles in a 28 kV Mo/Mo beam. As mentioned above, 2 mm of Al filtration was added for measurements with the RZ 1002/21 dosimeter. Data reveal that all dosimeters tested demonstrate varying degrees of angular dependence, with ionization chambers showing the least angular dependence and solid-state detectors showing the greatest dependence. Angular dependence data for the Barracuda MPD could only be collected for angles up to approximately  $\pm 35^\circ$  and  $\pm 50^\circ$  from normal for the vertical and horizontal alignments, respectively. Beyond this angular range, no discernable signal was recorded. Responses from all the dosimeters have a maximum at normal incidence and decrease with increasing angle; this trend is symmetric about normal incidence for all dosimeters except the Barracuda MPD. Coefficients of variation ( $CoV = \sigma/\mu$ ) for the raw data generally ranged from 0.0004 to 0.03. Error bars shown in the results span  $\pm(CoV \times y_N)$ , where  $y_N$  is the average signal normalized to perpendicular incidence.

Figure 5 shows the mean response as a function of absolute angle from normal incidence for each dosimeter, excluding the Barracuda MPD. Also shown are error bars indicating the standard deviation of the measurements and a fourth-order fit. Both the data and the fit are normalized to the fitted value at normal incidence ( $C_0$  from Equation 1). The Barracuda MPD response is shown in Figure 6. The data demonstrate both the limited range of the MPD and a strong angular asymmetry. Due to these observations, fits were not applied. Therefore, the results are shown normalized to the measured value at normal incidence and correction factors were not computed.

### 3.2 Ionization Chamber Model

The Fluke 96035B ion chamber was modeled with monoenergetic x-ray beams of between 10 and 24 keV. Figure 7b shows the model over varying monoenergetic beams, demonstrating the dependence of the angular trend on x-ray beam energy. Figure 7a shows the experimental results for 28 kV along with the model at 16 keV. At 16 keV, the model showed strong agreement with the experimental results obtained at 28 kV. The resulting mean absolute error was 0.009, averaged over all of the angles from  $0^\circ$  to  $90^\circ$ . Figure 7a also shows the response of a modeled ion chamber having infinitely thin walls/top, also calculated at 16 keV. There is a slight upward trend in the signal with angle due to the inverse square law.

### 3.3 Energy dependence

A smaller, coarser angular range was used to measure the signal from each dosimeter over varying beam quality. An angular range of  $\pm 45^\circ$  was chosen (excluding the Barracuda MPD), and the resulting measurements were consistently symmetric about normal incidence. These data were then used to analyze the kV dependence of the angular trends.

Results from the *t*-test and binomial counting showed that, as expected, lower beam energy generally produced a lower normalized value at a given angle. This pattern is attributed to non-normal incidence for all dosimeter types, as well as to beam hardening by the walls and top of the ionization chambers. The pattern is clear with the R100B and the RZ 1002/21 ( $p < 0.01$ ), and is present but less obvious with the ionization chambers ( $p > 0.05$ ). As an example, Figure 8 shows the relative response of the Barracuda R100B at  $45^\circ$  over varying tube voltage. The energy dependence for both orientations of the Barracuda MPD were irregular, and again no further analysis was conducted.

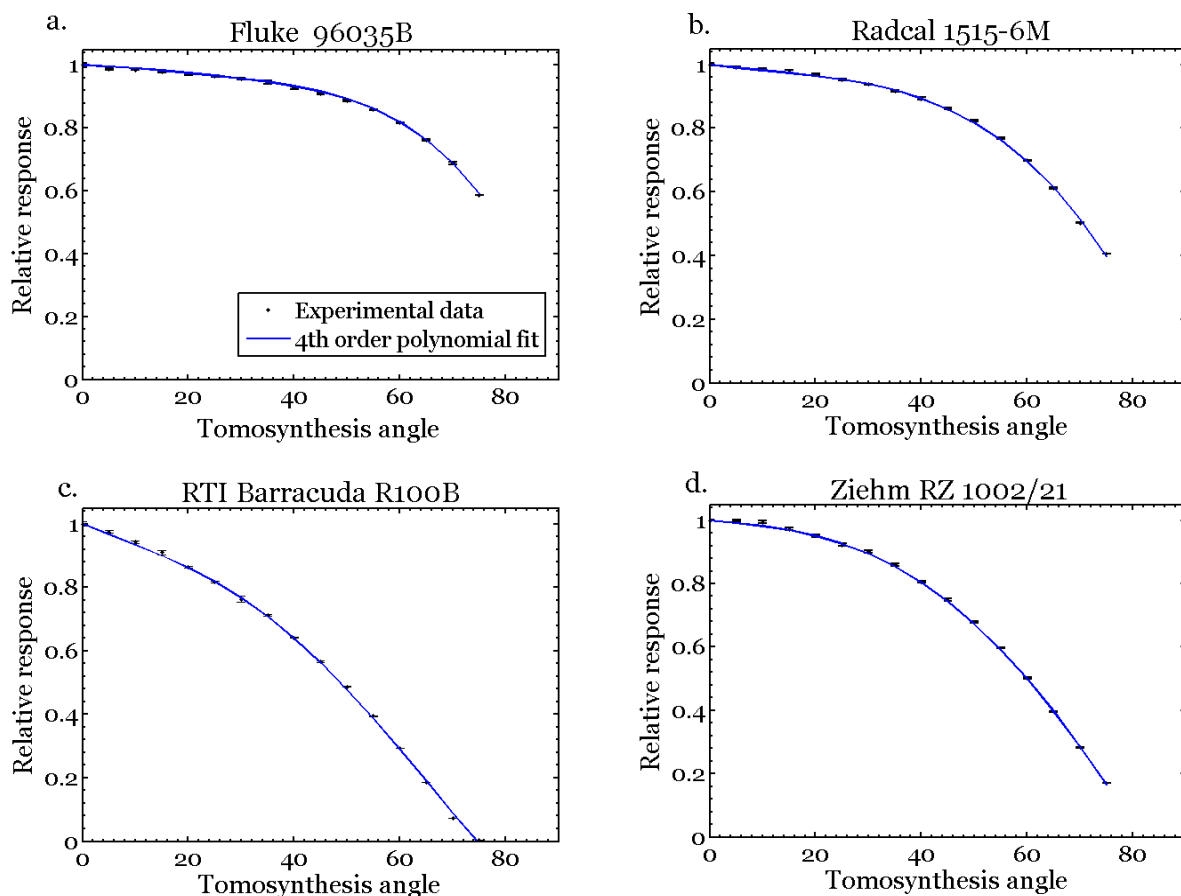


**Figure 5.** Normalized experimental response and 4th-order polynomial fit for a) Fluke 96035B, b) Radcal 1515-6M, c) RTI Barracuda R100B, and d) Ziehm RZ1002/21 dosimeters. Fitting coefficients are specified in Table 1. Note that in d), the RZ 1002/21 was exposed with an added 2 mm of Al filtration. All four figures implicitly share a common legend.

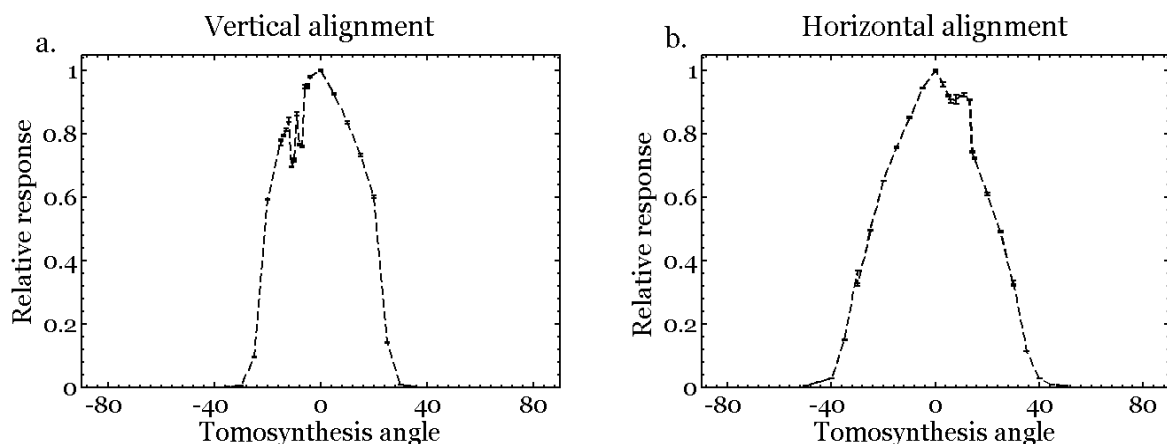


**Figure 6.** Normalized experimental response for a) vertical and b) horizontal alignment of Barracuda MPD showing the asymmetries of the response.

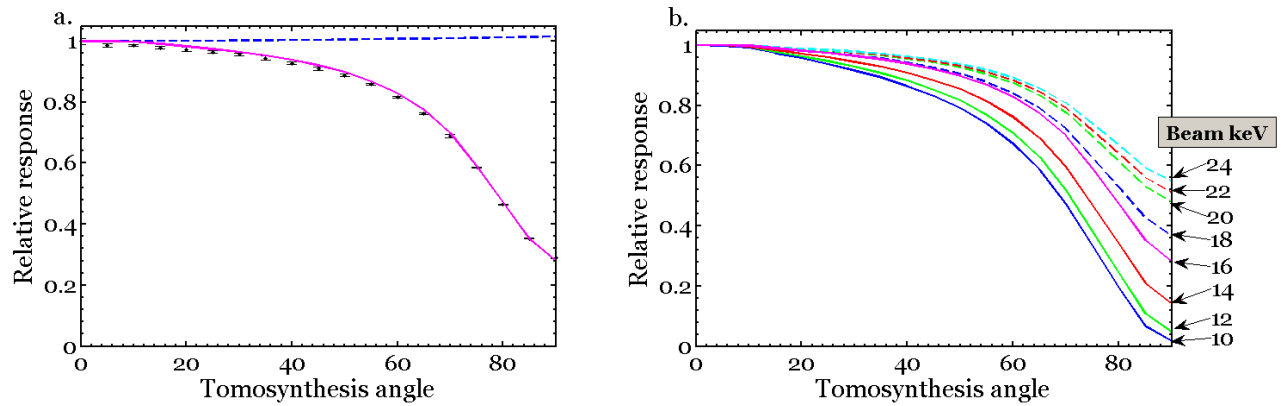


**Figure 7.** a) Normalized signal comparing experimental results (points with error bars) with an infinitely thin-walled version of Fluke 96035B chamber (dashed line) and a realistic model of the chamber (solid line) at 16 keV. b) Normalized signal from the realistic model of the Fluke 96035B ion chamber in monoenergetic beams ranging from 10 to 24 keV.

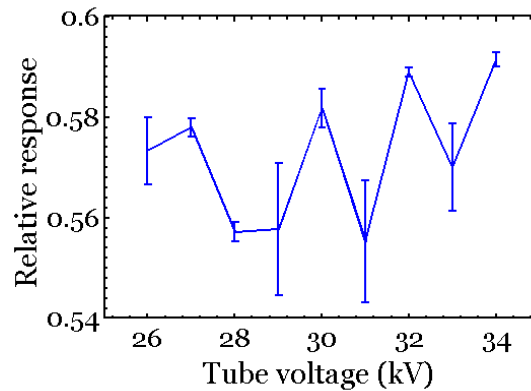


**Figure 8.** Relative response of the Barracuda R100B at an angle of 45° for various tube voltages. The plot demonstrates a slight energy dependence of the angular trend.

### 3.4 Correction factors

The responses of each dosimeter at 28 kV were fitted. In all cases, a fourth-order polynomial proved most appropriate. These fits, normalized to the fitted value at perpendicular incidence, are specified in Table 2 along with the corresponding coefficient of determination.

**Table 1.** Normalized coefficients of 4th-order, polynomial fit and coefficient of determination for each dosimeter, excluding Barracuda MPD. These fits are pictured in Figure 5.

Dosimeter	$C_0 / C_0$	$C_1 / C_0$	$C_2 / C_0$	$C_3 / C_0$	$C_4 / C_0$	$R^2$
96035B	1.000e+00	-3.685e-04	-7.577e-05	2.223e-06	-2.820e-08	0.99944
1515-6M	1.000e+00	-2.139e-03	4.603e-05	-1.260e-06	-5.386e-09	0.99934
R100B	1.000e+00	-7.156e-03	9.919e-05	-5.023e-06	3.445e-08	0.99956
RZ 1002/21	1.000e+00	-1.684e-03	1.545e-05	-3.006e-06	1.495e-08	0.99975

Using the equation coefficients specified in Table 1, correction factors were computed assuming an isocentric system where each view receives equal dose in the 28 kV Mo/Mo beam. Selected correction factors are shown in Table 2 for various DBT geometries specified by the number of views and the total angular range. Note that the magnitude of the correction factors (and hence the dosimetry error) decreases with increasing number of views in the DBT scan but increases as the total angular range increases.

**Table 2.** Select isocentric correction factors for the five dosimeters in a 28 kV, Mo/Mo beam generated using Equation 2. Note that an extra 2 mm of Al filtration was used in exposing the RZ 1002/21.

Dosimeter	Angular Range ( $\pm^\circ$ from normal)	Number of Views					
		3	9	11	15	25	49
<b>96035B</b>	5	1.0020	1.0016	1.0015	1.0015	1.0014	1.0014
	10	1.0046	1.0036	1.0035	1.0034	1.0033	1.0032
	15	1.0077	1.0059	1.0058	1.0056	1.0054	1.0053
	20	1.0114	1.0086	1.0084	1.0081	1.0078	1.0076
	25	1.0158	1.0116	1.0113	1.0110	1.0106	1.0103
<b>1515-6M</b>	5	1.0065	1.0055	1.0054	1.0053	1.0052	1.0051
	10	1.0122	1.0105	1.0103	1.0101	1.0099	1.0097
	15	1.0178	1.0152	1.0150	1.0147	1.0144	1.0141
	20	1.0240	1.0202	1.0198	1.0194	1.0189	1.0186
	25	1.0319	1.0258	1.0253	1.0246	1.0239	1.0234
<b>R100B</b>	5	1.0231	1.0194	1.0191	1.0187	1.0182	1.0179
	10	1.0463	1.0387	1.0380	1.0372	1.0362	1.0356
	15	1.0716	1.0590	1.0578	1.0565	1.0550	1.0539
	20	1.1014	1.0814	1.0797	1.0776	1.0754	1.0738
	25	1.1380	1.1070	1.1045	1.1016	1.0984	1.0961
<b>RZ 1002/21</b>	5	1.0056	1.0047	1.0046	1.0045	1.0044	1.0043
	10	1.0122	1.0098	1.0096	1.0094	1.0091	1.0089
	15	1.0212	1.0161	1.0157	1.0153	1.0148	1.0144
	20	1.0339	1.0243	1.0236	1.0228	1.0220	1.0213
	25	1.0516	1.0351	1.0339	1.0326	1.0312	1.0302



#### 4. DISCUSSION AND CONCLUSION

As DBT becomes more clinically prevalent, the development of DBT dosimetry is essential. It may be possible to apply mammographic dosimeters with DBT systems, but any errors involved in this move must first be well understood. Therefore, because DBT introduces rotation between the x-ray tube and dosimeter, this study investigated the dependence of mammographic dosimeters on their orientation relative to the incident beam.

In order to simulate an isocentric DBT system, five mammographic dosimeters were rotated relative to a Mo/Mo beam at various energies. The dosimeters studied included two ionization chambers, two solid-state detectors, and one photodiode. One ionization chamber was also selected and modeled in monoenergetic beams to further study the energy dependence of the angular trends.

The resulting data reveal that all dosimeters have some dependence on the angle of radiation incidence. For all dosimeters, the signal is maximized at normal incidence and decreases with increasing angle. Therefore, all of the dosimeters will underestimate the total dose if used with DBT. The magnitude of the angular dependence, however, is not consistent; solid-state detectors have the greatest angular dependence and ionization chambers have the least.

While most dosimeters show relatively predictable trends, the response from the Barracuda MPD was both strong and asymmetric. This is the result of attenuation and scatter from the internal construction of the device, seen in Figure 1. For this reason, solid-state dosimeters such as the Barracuda MPD should not be used for measuring the entrance air kerma integrated over a DBT scan. However, RTI Electronics does provide an ionization chamber as an alternative to the MPD. Although this device was not tested, it is likely that the response is similar to the ionization chambers tested in this work.

In fitting the angular dependence for dosimeter at 28 kV, a fourth-order polynomial proved to be most appropriate. Note, however, that each device had a unique fit; no one fit applied to all of the dosimeters. Using the fourth-order fits, sample correction factors were computed for each dosimeter to offset the total error involved with calculating integrated dose in DBT images. These factors reveal a large range of errors, from 0.1% to 14%, when using radiation incidence angles of up to  $\pm 25^\circ$  from the normal. As a result, the dosimetry error in DBT depends on both the angular range and the total number of projections.

The IAEA provides an example uncertainty budget that includes dosimeter errors between 0.3% and 1.0%.<sup>3</sup> With this as a guide, it may be appropriate in some situations to absorb the cumulative error from tube rotation into other uncertainties. Often, however, the angular error far exceeds this error budget; in these cases, it should not be ignored. If mammographic dosimeters are to be used, the correction factor appropriate to the dosimeter and imaging system should be applied.

Measurements of the angular dependence reveal that the trends, and thus the correction factors, are also dependent on beam energy. The 96035B ionization chamber's numerical model matched experimental results well by accounting for the inverse square law of intensity and any attenuation of the beam by the material of the chamber walls and top. However, attenuation in a medium, and therefore the attenuation coefficient used in the model, is known to be dependent upon the x-ray energy. As a result, although the model assumed exposure in a monoenergetic beam, it was sufficient to reveal energy dependence in the trends. At 16 keV, the model was a good approximation of the experimental data, but it lost agreement rapidly with energy. Also, an analysis of the experimental trends over varying tube voltage revealed similar energy dependence. A future goal is to study this trend in more detail by incorporating various x-ray spectra into the model. Regardless, any correction factor will need to be calculated for a specific beam energy and filtration.

It must be noted that the experiment and model were all performed assuming an isocentric DBT system, where the beam axis always passes directly through the center point of the dosimeter's top face. In commercial systems, this is rarely the case. Instead, the dosimeter and breast support may be slightly above or below the x-ray tube's center of rotation. In these situations, the distance between the dosimeter and x-ray tube varies, thus changing the effect of the inverse square law. In addition, the angle of radiation incidence at the dosimeter is related but no longer equal to the angle of tube rotation. Furthermore, moving the dosimeter so that it is not centered over the detector will alter the conditions further, varying the distance to the tube and increasing the incidence angle by up to  $17^\circ$ .<sup>5</sup> All of these factors influence the dosimeter signal and, consequently, the correction factors.

Combined, the results reveal that, when applied to DBT, mammographic dosimeters will underestimate the total dose received to the entrance surface of the breast. The signal measured using a mammographic dosimeter depends on the

type of dosimeter being used, the angle of radiation incidence, and the energy of the beam. In some limited cases, the error introduced may be small enough to be absorbed into other uncertainties. When this is not possible, though, correction factors must be customized to the specific imaging situation in order to be accurate. Among other things, this includes taking into account the dosimeter model, the beam energy as determined by the x-ray tube kV, target, and filtration, and the incidence angle and distance to the x-ray source as determined by geometry of the DBT system. In developing DBT dosimetry, a better solution would be to use an angle-independent dosimeter designed specifically for this modality.

### ACKNOWLEDGEMENTS

The authors would like to acknowledge the assistance of Raymond Acciavatti in the preparation of this paper. Financial support for this work has been provided by Hologic, Inc. (Bedford, MA) and the American Association for Physicists in Medicine (AAPM). Lena Bradley was supported in part by the AAPM Summer Undergraduate Fellowship Program. The contents of this paper are solely the responsibility of the authors and do not necessarily represent the official views of the Hologic or the AAPM.

### REFERENCES

- [1] Niklason, L.T., et al., "Digital Tomosynthesis in Breast Imaging," *Radiology* 20, 399-406 (1997).
- [2] Rafferty, E. A., "Tomosynthesis: New Weapon in Breast Cancer Fight," *Decisions in Imaging Economics*, 17 (2004).
- [3] IAEA, [Dosimetry in Diagnostic Radiology: An International Code of Practice], IAEA, Vienna, 41-81 (2007).
- [4] Fluke Biomedical, "10100AT TRIAT TnT Field Service Kit Operators Manual". Fluke Corporation, Cleveland, Ohio (2006).
- [5] Hajdok, G. and Cunningham, I. A., "Penalty on the detective quantum efficiency from off-axis incident x rays," *Proc. SPIE* 5368, 109-118 (2004).